



HAL
open science

Phylogenetic comparative approach reveals evolutionary conservatism, ancestral composition, and integration of vertebrate gut microbiota

Benoît Perez-Lamarque, Guilhem Sommeria-Klein, Loréna Duret, Hélène Morlon

► To cite this version:

Benoît Perez-Lamarque, Guilhem Sommeria-Klein, Loréna Duret, Hélène Morlon. Phylogenetic comparative approach reveals evolutionary conservatism, ancestral composition, and integration of vertebrate gut microbiota. *Molecular Biology and Evolution*, 2023, 10.1093/molbev/msad144 . hal-04133633

HAL Id: hal-04133633

<https://hal.sorbonne-universite.fr/hal-04133633>

Submitted on 20 Jun 2023

HAL is a multi-disciplinary open access archive for the deposit and dissemination of scientific research documents, whether they are published or not. The documents may come from teaching and research institutions in France or abroad, or from public or private research centers.

L'archive ouverte pluridisciplinaire **HAL**, est destinée au dépôt et à la diffusion de documents scientifiques de niveau recherche, publiés ou non, émanant des établissements d'enseignement et de recherche français ou étrangers, des laboratoires publics ou privés.



Distributed under a Creative Commons Attribution 4.0 International License

1 **Phylogenetic comparative approach reveals evolutionary**
2 **conservatism, ancestral composition, and integration of vertebrate**
3 **gut microbiota**

4
5
6 Benoît Perez-Lamarque ^{1,2*} (ORCID: 0000-0001-7112-7197)

7 Guilhem Sommeria-Klein ³ (ORCID: 0000-0002-5331-3639)

8 Loréna Duret ¹ (ORCID: 0000-0001-7031-4900)

9 Hélène Morlon ¹ (ORCID: 0000-0002-3195-7521)

10
11
12 ¹ *Institut de biologie de l'École normale supérieure (IBENS), École normale supérieure,*
13 *CNRS, INSERM, Université PSL, 46 rue d'Ulm, 75 005 Paris, France*

14
15 ² *Institut de Systématique, Évolution, Biodiversité (ISYEB), Muséum national d'histoire*
16 *naturelle, CNRS, Sorbonne Université, EPHE, UA, CP39, 57 rue Cuvier 75 005 Paris,*
17 *France*

18
19 ³ *Department of Computing, University of Turku, Yliopistonmäki, 20014 Turku, Finland*

20
21 *Correspondence: Benoît Perez-Lamarque (benoit.perez@ens.psl.eu)

22 **Abstract:**

23

24 How host-associated microbial communities evolve as their hosts diversify remains
25 equivocal: How conserved is their composition? What was the composition of ancestral
26 microbiota? Do microbial taxa covary in abundance over millions of years? Multivariate
27 phylogenetic models of trait evolution are key to answering similar questions for
28 complex host phenotypes, yet they are not directly applicable to relative abundances,
29 which usually characterize microbiota. Here, we extend these models in this context,
30 thereby providing a powerful approach for estimating phylosymbiosis (the extent to
31 which closely related host species harbor similar microbiota), ancestral microbiota
32 composition, and integration (evolutionary covariations in bacterial abundances). We
33 apply our model to the gut microbiota of mammals and birds. We find significant
34 phylosymbiosis that is not entirely explained by diet and geographic location, indicating
35 that other evolutionary-conserved traits shape microbiota composition. We identify
36 main shifts in microbiota composition during the evolution of the two groups and infer
37 an ancestral mammalian microbiota consistent with an insectivorous diet. We also find
38 remarkably consistent evolutionary covariations among bacterial orders in mammals
39 and birds. Surprisingly, despite the substantial variability of present-day gut microbiota,
40 some aspects of their composition are conserved over millions of years of host
41 evolutionary history.

42

43

44 **Keywords:**

45

46 gut microbiome, interactome, phylosymbiosis, holobiont evolution, phylogenetic signal,
47 comparative methods.

48 **Introduction:**

49

50 Host-associated microbial communities, referred to as the *microbiota*, often play
51 central roles in the biology of the hosts and their interactions with the environment. As
52 host clades diversify, the microbiota can furthermore play a key role in the adaptation
53 of their hosts to different ecological conditions. This raises important questions on the
54 evolution of the microbiota as hosts diversify. First, how much is microbiota
55 composition conserved over host evolutionary timescales? While the microbiota can
56 be quite labile within and between host species (Ley et al. 2008; David et al. 2014;
57 Hacquard et al. 2015; Hird et al. 2015; Amato et al. 2019), more closely related host
58 species often tend to have more similar microbiota, a pattern referred to as
59 *phylosymbiosis* (Brooks et al. 2016; Lim and Bordenstein 2020). In animals, levels of
60 phylosymbiosis appear to be heterogeneous across tissues (e.g. gut or skin
61 microbiota) and lineages (Mazel et al. 2018; Lim and Bordenstein 2020; Song et al.
62 2020; Perez-Lamarque, Krehenwinkel, et al. 2022).

63

64 The presence of a phylogenetic signal in microbiota composition across hosts
65 could potentially be used to reconstruct ancestral microbiota composition. Ancestral
66 reconstructions could be particularly useful to detect events during host diversification
67 associated with major shifts in microbiota composition or to verify hypotheses on
68 ancestral diets. A phylogenetic signal in microbiota composition may also inform on
69 potential long-term evolutionary covariations in abundances between microbial taxa.
70 Positive or negative covariations may arise from direct interactions between microbial
71 taxa, such as cross-feeding, trophic relationships, or competition (Faust et al. 2012;
72 Foster et al. 2017; Kohl 2020), or from (anti)correlated responses to variations in the
73 environment (e.g. similar or opposite responses to decreased pH). We refer to these
74 covariations as *microbiota integration* by analogy with the often observed *phenotypic*
75 *integration* between traits in complex phenotypes (Pigliucci 2003). Such covariations
76 would indicate constraints in the evolution of microbiota composition.

77

78 Phylogenetic comparative methods offer a rich toolbox for quantifying
79 phylogenetic signal, reconstructing ancestral states, and detecting integration in
80 multidimensional phenotypes (Clavel et al. 2015). These methods rely on modeling the
81 evolution of a set of phenotypic traits across evolutionarily related species through a
82 multivariate stochastic process, such as the Brownian motion process, running along
83 the species' phylogenetic tree (Revell et al. 2008; Harmon 2017). The multivariate
84 Brownian process models the gradual evolution of traits through the accumulation of
85 stochastic changes drawn from a multivariate normal distribution with a variance-
86 covariance matrix that reflects the magnitude of the changes for each trait (the variance
87 terms) and the covariation in the changes between trait pairs (the covariance terms).
88 This process is relevant to represent long-term variations in the abundances of the
89 different microbial taxa that constitute the microbiota, as such variations are an
90 emerging outcome of: (i) the stochastic accumulation of changes in the numerous host
91 traits that can influence the microbiota, including both extrinsic (e.g. geographic

92 location, habitat) and intrinsic (e.g. diet, antimicrobial excretions) traits (Moran et al.
93 2019; Kohl 2020; Lim and Bordenstein 2020) and (ii) interactions between microbial
94 taxa (Foster et al. 2017). Indeed, the Brownian motion process has already been used
95 to model variations in microbial abundances over host evolutionary time (Capunitan et
96 al. 2020; Labrador et al. 2021). However, the process is not directly applicable to
97 compositional data made of relative microbial abundances as it does not constrain its
98 components to sum to 1, and absolute abundances are unfortunately typically not
99 provided by mainstream metabarcoding technics used to characterize microbiota
100 composition. Thus, current phylogenetic comparative methods cannot directly be used
101 in the context of microbiota evolution without transgressing several model assumptions
102 (Hird 2019).

103

104 Here, we develop an approach to apply the multivariate Brownian motion
105 process to compositional data. We also include a widely-used tree transformation
106 (Pagel 1999) that quantifies phylosymbiosis by evaluating how much host phylogeny
107 contributes to explaining interspecific variation in present-day microbiota composition.
108 Phylosymbiosis is typically assessed using correlative approaches such as Mantel
109 tests (Lim and Bordenstein 2020), which are known to suffer from frequent false
110 negatives, while process-based approaches such as ours tend to be more powerful
111 (Harmon and Glor 2010; Hird 2019; Perez-Lamarque, Maliet, et al. 2022). We apply
112 our new approach to the gut bacterial microbiota of mammals and birds. The gut
113 microbiota is key to the functioning of their hosts, contributing to their nutrition, their
114 protection, and their development (McFall-Ngai et al. 2013). Strong phylosymbiosis in
115 gut bacterial microbiota has been reported for mammals, including primates and
116 rodents (Ochman et al. 2010; Groussin et al. 2017; Kohl et al. 2018), while it is thought
117 to be absent for birds, with some exceptions in a few young clades (Song et al. 2020;
118 Trevelline et al. 2020; Bodawatta et al. 2022). We revisit this dichotomy here, on the
119 premise that previous analyses may have not been powerful enough to detect
120 phylosymbiosis in birds (Hird 2019). We analyze potential drivers of phylosymbiotic
121 patterns, including diet, geographic location, and flying ability, we estimate the
122 ancestral microbiota composition of mammals and birds, and we investigate patterns
123 of microbiota integration.

124 Results & Discussion:

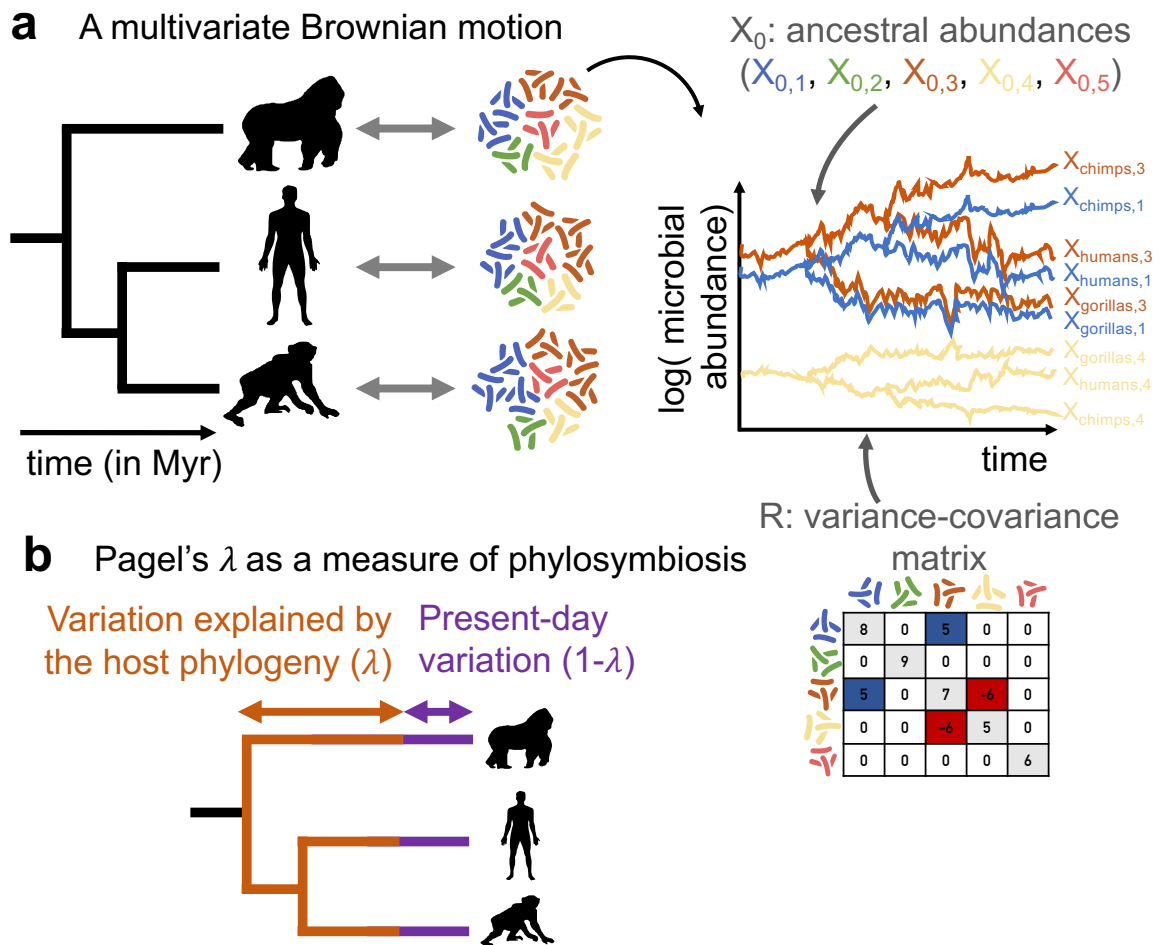
125

126 We developed a method to infer the dynamics of microbiota composition during
127 host diversification from host-microbiota data (*i.e.* a fixed, bifurcating host phylogeny
128 and microbiota relative abundances for each extant host species) using the
129 multivariate Brownian motion process (Figure 1 and Methods). We assume that all
130 microbial taxa are present in all hosts, potentially in very low (undetectable)
131 abundances and that they were already present in the most recent common ancestor
132 of all host species. These assumptions are met if we consider a taxonomic level in the
133 definition of microbial taxa that is high enough given the host clade, such as bacterial
134 orders in the vertebrate gut microbiota. We assume that, from ancestral values at the
135 root X_0 , the log-absolute abundances of the different microbial taxa change on the host
136 phylogeny following a multivariate Brownian motion model with variance-covariance
137 matrix R (Figure 1a). Under this model, the log-absolute abundances fluctuate around
138 their ancestral values ($\log X_0$) without directional change. In addition, we account for
139 variation linked to present-day factors by including in the model the widely-used
140 Pagel's λ transformation of the host phylogenetic tree (Pagel 1999). This
141 transformation extends the terminal branches of the tree by $(1-\lambda)$ of the total tree depth
142 while compressing the internal branches to keep the total tree depth constant, with λ
143 ranging between 0 and 1 (see Figure 1b and Methods). λ estimates close to 1 indicate
144 that an untransformed tree explains the data quite well, reflecting strong
145 phylosymbiosis, whereas λ estimates close to 0 indicate that the tree has little
146 explanatory power, reflecting weak or absent phylosymbiosis. Unlike the traditional
147 case of the multivariate Brownian motion process applied to phenotypic data, where
148 the phenotype is directly measured at present, in the case of the microbiota, relative
149 rather than absolute abundances are measured. To handle this difficulty, we treat total
150 microbial abundances in each host as latent variables, and sample from the joint
151 posterior distribution of these latent variables and our parameters of interest: Pagel's
152 λ , which provides us with an estimate of phylosymbiosis, the R matrix which reflects
153 microbiota integration, and Z_0 , which indicates the relative microbial abundances in the
154 ancestral microbiota.

155

156 We tested this inference method on data simulated from our model and found
157 that we can accurately estimate the ancestral bacterial relative abundances Z_0 (with a
158 tendency for homogenization) and the variance-covariance matrix R between microbial
159 taxa, provided that the number of host species (n) and bacterial taxa (p) are large
160 enough ($n \geq 50$ and $p \geq 5$, see Supplementary Results 1). Similarly, the level of
161 phylosymbiosis λ is accurately estimated for $p \geq 5$, and its significance is correctly
162 inferred for $n \geq 50$ (see Supplementary Results 1). This approach provides a more
163 powerful way to detect phylosymbiosis than Mantel tests, which often failed at
164 detecting low levels of phylosymbiosis ($0 < \lambda < 0.5$; Table S1). This was expected, as
165 Mantel tests are correlative and are known to suffer from frequent false negatives in

166 comparison with more process-based approaches such as ours (Harmon and Glor
 167 2010; Hird 2019; Perez-Lamarque, Maliet, et al. 2022).
 168
 169



170
 171
 172 **Figure 1: A comparative phylogenetic model for the dynamics of microbiota**
 173 **composition during host diversification:** (a) We model fluctuations in the abundances of
 174 microbial taxa along a host phylogeny with a multivariate Brownian motion parametrized by
 175 the ancestral abundances (X_0) and the variance-covariance matrix (R). The variance terms (on
 176 the diagonal) reflect the magnitude of the changes, while the covariance terms reflect positive
 177 or negative covariations in abundances between pairs of microbial taxa. The relative ancestral
 178 abundances (Z_0) and the variance-covariance matrix R are estimated by adjusting the model
 179 to the host-microbiota data (host phylogeny and microbiota relative abundances for each host).
 180 (b) Following the widely-used Pagel's λ transformation, we extend the terminal branches of
 181 the host phylogenetic tree by $1-\lambda$ of the total tree depth while compressing the internal
 182 branches to keep the total tree depth constant. λ is comprised between 0 and 1 and is co-
 183 estimated during inference. λ close to 1 indicates that closely related hosts tend to have similar
 184 microbiota due to shared evolutionary history (strong phyllosymbiosis), while λ close to 0
 185 indicates that microbiota composition is determined by present-day processes with little
 186 influence of host evolutionary history (weak or absent phyllosymbiosis). The significance of
 187 phyllosymbiosis is assessed with permutations.

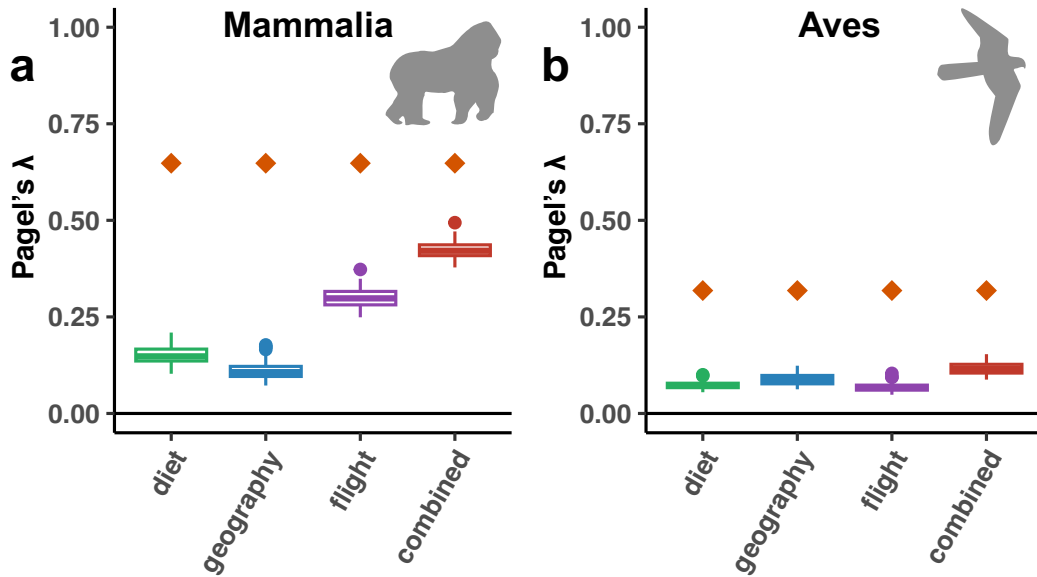
188 We applied our model to the gut bacterial microbiota of 215 mammal species
189 and 323 bird species from (Song et al. 2020) and found a pervasive signal of
190 phylosymbiosis. We focused on the 14 most abundant bacterial orders, corresponding
191 in abundance to 84% and 82% of the total gut bacterial microbiota of mammals and
192 birds, respectively. We found a markedly higher level of phylosymbiosis in mammals
193 ($\lambda \approx 0.65$) than in birds ($\lambda \approx 0.31$; Table S2, Figure S1), consistent with previous
194 literature and our finding that microbiota composition is more species-specific in
195 mammals than in birds (Table S3). Indeed, bird microbiota is generally more sensitive
196 to short-term environmental changes such as anthropogenic perturbations or parasite
197 infections (Bodawatta et al. 2022). By explicitly modeling the non-phylogenetic
198 component of microbiota composition using a Pagel's λ transformation, we detected a
199 low but significant level of phylosymbiosis in the gut microbiota of birds (Table S2),
200 contrary to previous conclusions (Song et al. 2020; Bodawatta et al. 2022) that relied
201 on Mantel tests. λ values are higher at the level of bacterial phyla (Table S2; Figure
202 S1), suggesting that microbiota composition is more evolutionarily conserved at higher
203 taxonomic levels. Testing model performance on data simulated directly on the
204 mammal and bird phylogenetic trees, we found a low type-I error rate and a high
205 statistical power, suggesting that the phylosymbiosis we detected in birds is not due to
206 false detection by our method, but rather to a higher power than previously used
207 methods (Table S4). Phylosymbiosis is not linked to an effect of captivity nor the
208 spurious concatenation of different studies either (Supplementary Results 2).
209 Phylosymbiosis is particularly strong in Primates, Passeriformes, and Cetartiodactyla,
210 lower but significant in Columbiformes, Chiroptera, and Carnivora, and non-significant
211 in Rodentia, Charadriiformes, and Anseriformes (Table S2). Non-significant
212 phylosymbiosis in these orders is likely due to an insufficient number of sampled
213 species ($n < 25$, see Supplementary Results 1). It appears that vertebrate orders with
214 mainly herbivorous diets have stronger phylosymbiosis, although this would need to
215 be tested more robustly with a better species coverage (Table S2).

216
217 Our results suggest that phylosymbiosis is only partially explained by
218 evolutionary conservatism in flying ability, diet, or geographic location. First, excluding
219 flying mammals (Chiroptera) or non-flying birds did not impact our estimates of
220 phylosymbiosis (Table S2). Second, permutation tests shuffling the microbiota of host
221 species having the same diet, geographic location, flying ability, or combination of
222 these traits resulted in much lower λ values (Figures 2 & S2). In mammals, λ values
223 resulting from such shuffling are still significant (Figure 2), suggesting that the
224 evolutionary conservatism of flying ability, diet, and geographic location contributes to
225 phylosymbiosis without fully explaining it (Moran et al. 2019). In birds, shuffling often
226 resulted in non-significant λ values (Figure 2), indicating a weak or absent contribution
227 of diet or geographic location in the observed phylosymbiosis. Similarly, the
228 conservatism of these traits is not sufficient to explain the phylosymbiosis measured in
229 some of the larger mammal and bird clades, such as Primates, Cetartiodactyla, and
230 Passeriformes (Figure S3). Thus, we suspect that other evolutionary-conserved

231 physiological, immunological, or ecological traits act as host filters (Foster et al. 2017;
232 Moran et al. 2019) and contribute to phyllosymbiosis in the gut microbiota of mammals
233 and birds (Goodrich et al. 2016; Mazel et al. 2018).

234

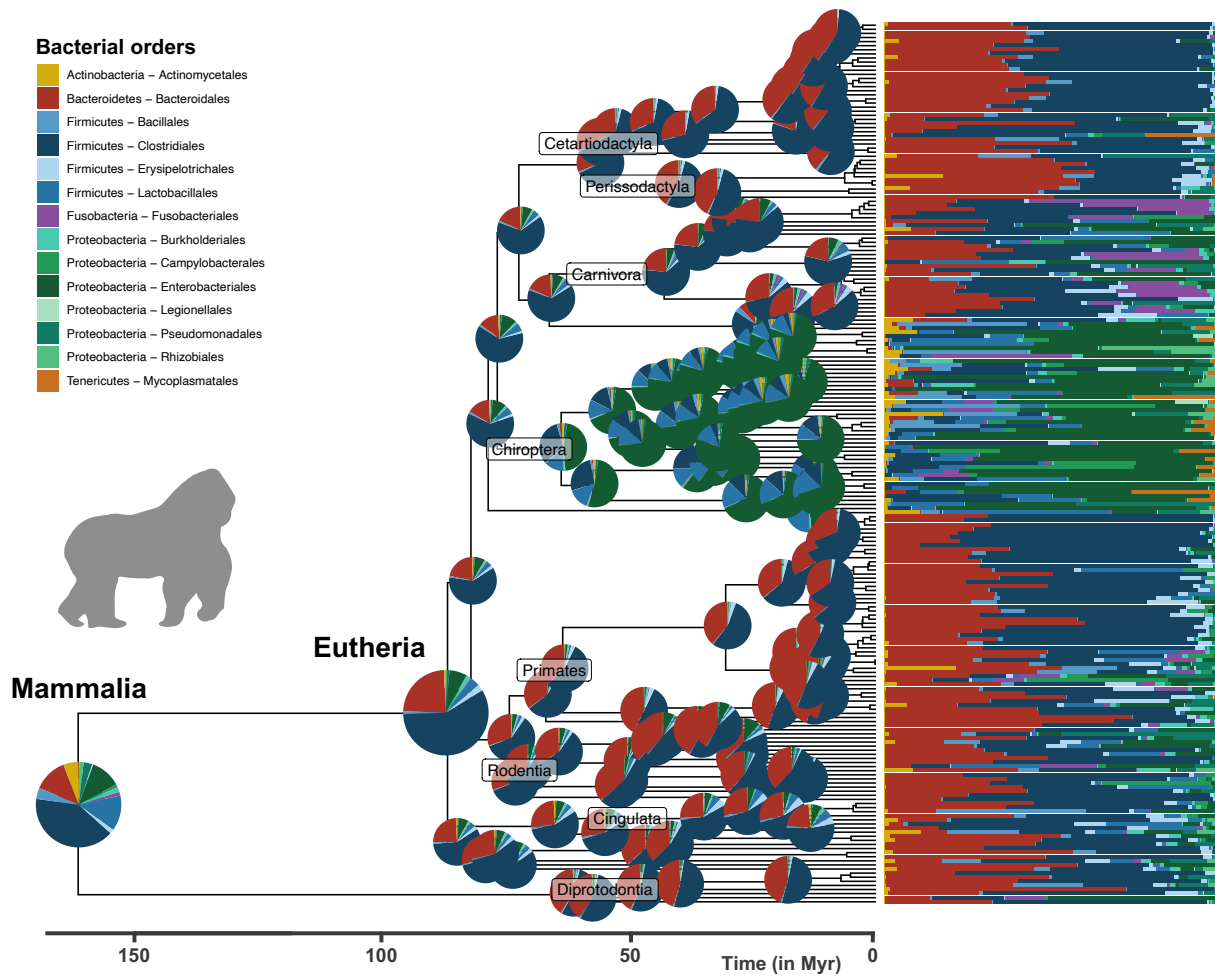
235 Our ancestral reconstructions of the microbiota of early mammals and birds
236 suggest that Proteobacteria and Firmicutes were much more abundant in the ancestral
237 gut microbiota of birds than mammals (Figures 3, 4, S4 & S5). As common in
238 phylogenetic ancestral reconstruction, the uncertainty is quite high (Figure S6); it is
239 larger in mammals than in birds because of the long branches that separate marsupials
240 and eutherians at the origin of all mammals. In the absence of fossil constraints,
241 ancestral reconstructions are a phylogenetically-weighted average of extant
242 characteristics. Estimated ancestral compositions are thus expectedly close from the
243 average microbiota compositions of extant bird and mammal species, yet they are
244 distinct (Figure S7). Comparing the ancestral microbiota composition of mammals to
245 that of the extant wild mammal species, we found the highest similarity with
246 invertebrate feeders (distance to the centroid: $d=1.46$), such as the insectivorous
247 armadillos (*Zaedyus pichiy*), and frugivores ($d=1.24$; Figures 5 & S8; see Methods),
248 and the lowest similarity with specialist consumers feeding on plants ($d=2.50$) or meat
249 ($d=2.82$). This result is robust to uncertainty in our estimate of ancestral microbiota
250 composition (Figure S6b) and when including species sampled in captivity (Figure S7).
251 Given that mammals originated before fleshy fruit plants (Eriksson 2016), this suggests
252 that ancestral mammals were generalist invertebrate feeders, which is consistent with
253 the current hypothesis, based on the fossil record and ancestral diet reconstruction, of
254 a generalist insectivorous diet in early mammals (Gill et al. 2014; Grossnickle et al.
255 2019). We found the gut microbiota composition of modern birds to be only weakly
256 structured by diet compared to that of mammals, making the inferred ancestral
257 microbiota composition of birds less informative in this respect (no strong clustering in
258 the PCA plots; PerMANOVA testing the effect of diet: $R^2\sim 0.03$, $p<0.001$ in birds *versus*
259 $R^2\sim 0.22$, $p<0.001$ in mammals; Figures 5, S7 & S8; Table S5). In addition, the fact
260 that, under the assumptions of our model, most extant microbiota compositions in both
261 mammals and birds remain centered around the estimated ancestral microbiota
262 composition suggests that only a minority of the extant species experienced major
263 shifts in their microbiota composition during their evolution.



264
265

Figure 2: Phylogenetically-conserved diets, geographic locations, or flying abilities partially contribute to phylosymbiosis in the gut microbiota of mammals, but not birds.

268 For both mammals and birds, we compared the estimated level of phylosymbiosis (mean λ
269 value in orange) to levels of phylosymbiosis (λ values) estimated when shuffling the species
270 that have the same diet (green boxplot), geographic location (blue boxplot), flying ability (flying
271 or non-flying; purple boxplot), or combination of the latter traits (in red). For each shuffling
272 strategy, we performed 100 randomizations. Combining all traits strongly constrains the
273 possible permutations, which may consequently retain a phylogenetic signal in the shuffling
274 and lead to high λ values although the traits are actually not strongly contributing to
275 phylosymbiosis.



276

277

278

279

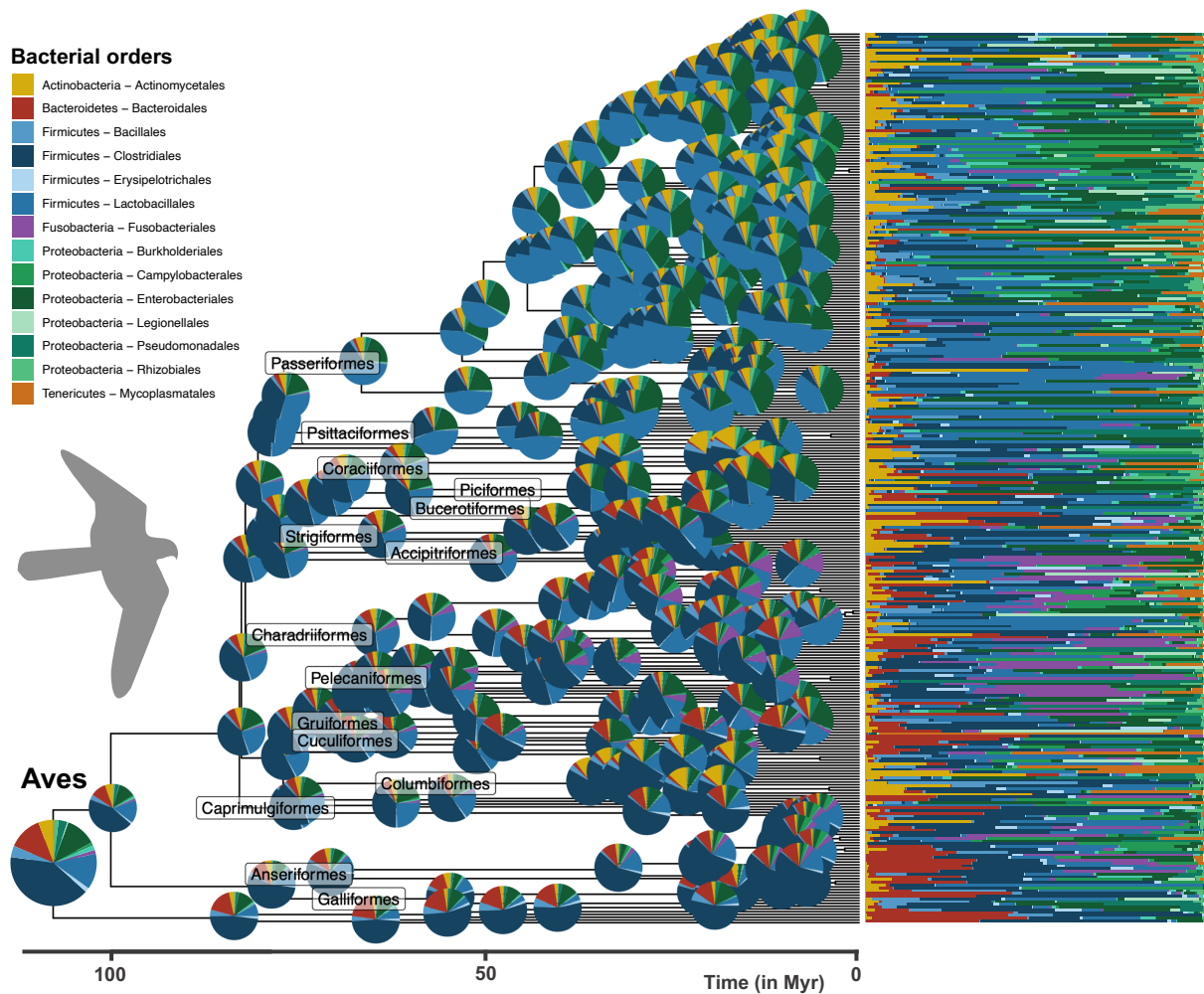
280

281

282

283

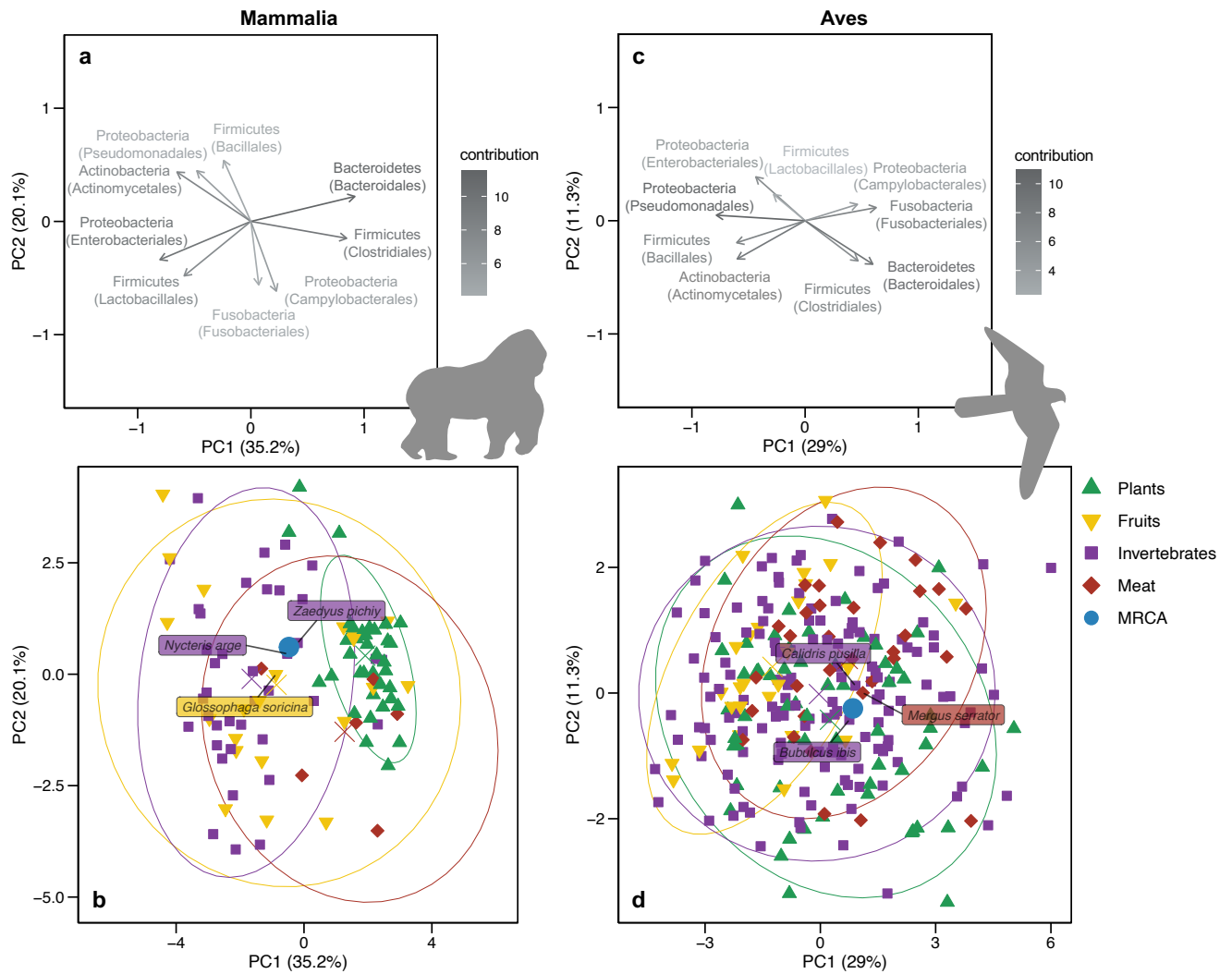
Figure 3: Ancestral reconstruction of mammalian gut microbiota: Phylogenetic tree of the sampled mammal species and associated relative abundances of the 14 most abundant bacterial orders (bar charts on the right). Pie charts at the root and nodes of the tree represent estimated ancestral microbiota compositions (mean of the posterior distribution of Z_0 at the root and generalized least squares estimates at other internal nodes). Compositions are not represented at the most recent nodes for the sake of clarity.



284
 285
 286
 287
 288
 289
 290
 291

Figure 4: Ancestral reconstruction of avian gut microbiota: Phylogenetic tree of the sampled birds, and associated relative abundances of the 14 most abundant bacterial orders (bar charts on the right). Pie charts at the root and nodes of the tree represent estimated ancestral microbiota compositions (mean of the posterior distribution of Z_0 at the root and generalized least squares estimates at other internal nodes). Compositions are not represented at the most recent nodes for the sake of clarity.

292 We detected significant changes in microbiota composition in the ancestors of
293 some mammal and bird orders (Figures 3, 4, & S9). In mammals, the largest shift in
294 microbiota composition occurred in the ancestor of Chiroptera, with an increased
295 proportion of Enterobacteriales (Proteobacteria), Mycoplasmatales (Tenericutes), and
296 to a lesser extent Actinomycetales (Actinobacteria), as well as a decreased proportion
297 of Bacteroidales (Bacteroidetes), and in Firmicutes, Clostridiales were replaced by
298 Bacillales and Lactobacillales (Figure 3; Table S6). Other shifts occurred in the
299 ancestor of Carnivora, with an increased proportion of Fusobacteriales (Fusobacteria),
300 and in the ancestors of Primates and Cingulata, with an increased proportion of some
301 Firmicutes orders (*e.g.* Erysipelotrichales; Figures 3 & S9). In addition, Proteobacteria
302 (especially Enterobacteriales and Pseudomonadales) almost disappeared in the
303 ancestral microbiota of Ungulata and Simiiformes (New and Old World monkeys; Table
304 S6). In birds, we found a shift in microbiota composition in the ancestor of
305 Passeriformes, with more Bacillales and Enterobacteriales, and to a lesser extent
306 Pseudomonadales, and a quasi-disappearance of Bacteroidales (Figures 4 & S5;
307 Table S6). The ancestors of Anseriformes and Charadriiforms were characterized by
308 a larger proportion of Bacteroidales, as well as a large proportion of Fusobacteriales,
309 often absent or present in low abundances in other bird gut microbiota. Finally, the
310 relative abundance of Actinomycetales increased in Columbiformes (Table S6). We
311 found similar estimates of ancestral gut microbiota composition when running separate
312 inferences for the different mammal and bird orders (Figure S9). Some of these
313 compositional shifts might be linked to the ecological changes that these lineages
314 experienced, such as the acquisition of flight for bats or carnivorous diets for Carnivora
315 and Charadriiforms (Nishida and Ochman 2018; Song et al. 2020).
316

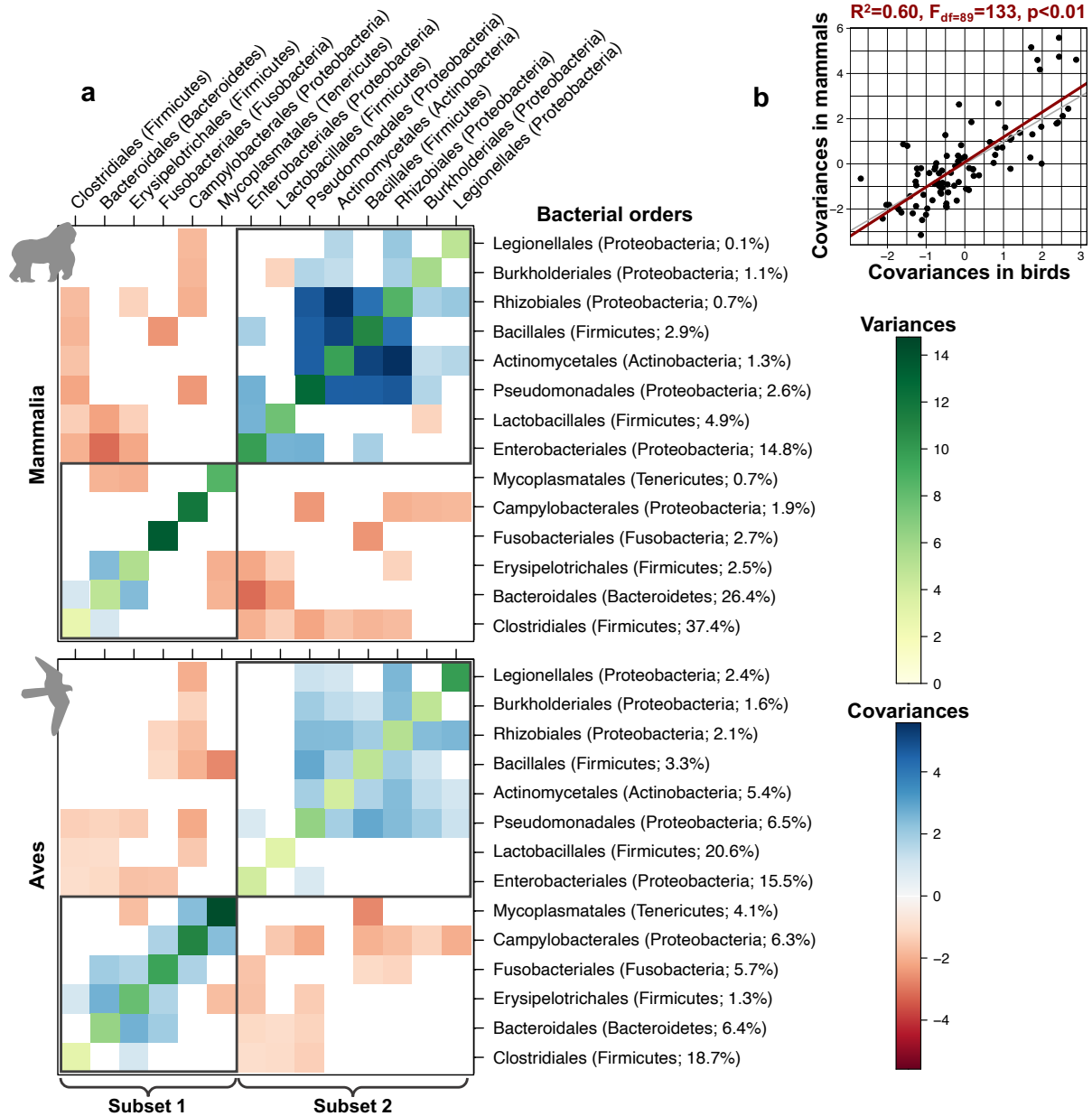


317
318

319 **Figure 5: Projection of the estimated ancestral gut microbiota of mammals and birds**
 320 **onto the space of present-day gut microbiota.** Top panels: projection of bacterial orders
 321 contributing to the two principal components (PC). Colors represent the contribution of the taxa
 322 to the principal components. Percentages indicate the explained variance of each PC. Only
 323 the 9 most abundant orders are represented for the sake of clarity. Bottom panels: Projection
 324 of the extant and ancestral microbiota compositions. Extant microbiota of species sampled in
 325 the wild are colored according to the species' diet. For each diet, the ellipse contains on
 326 average 95% of the distribution approximated by a multivariate t-distribution and the centroid
 327 is indicated by a diagonal cross. Ancestral microbiota compositions of mammals and birds are
 328 represented in blue. On each PCA plot, we indicated the three extant species with microbiota
 329 compositions closest to the ancestral microbiota composition. The ancestral gut microbiota of
 330 mammals is closest to the gut microbiota of present-day invertebrate feeders; the gut
 331 microbiota of birds does not strongly reflect diet.

332 Far from varying as uncorrelated units during the evolutionary history of
333 mammals and birds, we found significant covariances between many microbial taxa,
334 both positive and negative (Figure 6a), suggesting strong constraints in the evolution
335 of the microbiota. These patterns of microbiota integration are strikingly similar in
336 mammals and birds (Figure 6b), indicating that they are conserved over long
337 evolutionary times. Our simulation analyses on the mammal and bird trees suggest
338 that these results are not artefactual, since we recover significant covariances only
339 when we include them in the simulations (Table S7, Supplementary Results 1). Similar
340 covariances were obtained when performing separate inferences on the different
341 mammal and bird orders (Figure S10), which both confirms our results and suggests
342 that the model assumption of a constant variance-covariance matrix across the host
343 phylogenetic tree is reasonable. Combined with the high bacterial variability in time,
344 across individuals, and across host species at low taxonomic levels, these consistent
345 patterns at the level of bacterial orders on large time scales suggest that there is a
346 certain level of functional redundancy among bacteria taxa within orders in the
347 vertebrate gut microbiota.

348
349 Both visual inspection and integration analyses of the covariances revealed that
350 bacterial orders cluster into two main subsets within which taxa tend to covary in a
351 concerted way, while taxa from different subsets tend to be anti-correlated (Figure 6;
352 see Methods). The first subset (“subset 1”) is formed in particular by the orders
353 Clostridiales, Bacteroidales, and Fusobacteriales, and the second subset (“subset 2”)
354 is mainly composed of the orders Enterobacteriales, Lactobacillales, Pseudomonades,
355 Actinomycetales, and Bacillales. Although some host species have a microbiota
356 composed of an even mixture of these two bacterial subsets, one subset generally
357 prevails, leading to the existence of two main gut microbiota profiles. The first subset
358 is dominant in the microbiota of most mammals (excluding Chiroptera), the ancestors
359 of birds, and some extant bird lineages (*e.g.* Anseriformes, Columbiformes, or
360 Accipitriformes); the second subset predominates in the microbiota of Chiroptera and
361 other bird lineages, including Passeriformes (Figure S11). This result suggests the
362 existence of two main gut microbiota profiles conserved over millions of years across
363 vertebrates.



364

365

366

367

368

369

370

371

372

373

374

Figure 6: Estimated variances and covariances between the main bacterial taxa tend to be similar in the gut microbiota of mammals and birds. (a) For each variance-covariance matrix between bacterial taxa estimated using our model of host microbiota evolution, we represented negative covariances in red and positive covariances in blue, while variances are represented in shades of green. Non-significant covariances are represented in white. Grey rectangles correspond to subsets of bacterial orders that tend to covary positively. **(b)** Correlation between covariances between the main bacterial taxa estimated in the gut microbiota of mammals or birds. The red line indicates the corresponding linear model, while the grey line corresponds to $y=x$.

375 We can only speculate on the processes underlying positive or negative
376 covariances between bacterial orders: we cannot distinguish from our analyses
377 whether they indicate direct interactions between bacterial taxa (e.g. cross-feeding or
378 competition) or indirect interactions mediated by similar/opposed microbial responses
379 to changes in the gut environment. For instance, the frequent and strong negative
380 covariations observed between the abundant Enterobacteriales (Proteobacteria) and
381 the major bacterial orders Clostridiales (Firmicutes) and Bacteroidales (Bacteroidetes)
382 may result from direct competitions (Shealy et al. 2021), host immunological controls
383 over Proteobacteria (Mirpuri et al. 2013), and/or be mediated by the oxygen
384 concentration in the gut, as Proteobacteria are facultative anaerobes, while other phyla
385 are obligate anaerobes (Shin et al. 2015). The strongest positive covariations we
386 inferred between Actinomycetales, Pseudomonadales, and Rhizobiales, which are the
387 most abundant bacterial orders in plant tissues (Wagner et al. 2016), may reflect a
388 plant-based diet, which would lead to a concomitant increase of plant-associated
389 bacteria in the gut microbiota of herbivorous vertebrates (Dion-Phénix et al. 2021).
390 Some of the covariations we detected (e.g. the negative covariation between
391 Lactobacillales and Bacteroidales) have also been observed in human microbiome
392 data using co-occurrence network analyses (Faust et al. 2012), suggesting that at least
393 some covariations between microbial taxa that occur over short timescales within host
394 species are conserved over macroevolutionary timescales.

395
396 To test the adequacy of our model to the data, we simulated microbiota under
397 our model using the parameters estimated on mammal and bird data. We found that
398 simulated microbiota have compositions similar to those observed in extant mammals
399 and birds (Figure S12), which indicates that, despite its simple assumptions, our
400 multivariate Brownian motion model generates realistic gut microbiota (Hird 2019;
401 Labrador et al. 2021). Nevertheless, the gut microbiota composition of mammals and
402 birds appears more constrained than the sets of compositions we can simulate using
403 multivariate Brownian motions (Figure S12). This is particularly true for mammals and
404 may be linked to constraints that are not accounted for by our model, such as selective
405 pressures toward particular microbiota compositions, the potential existence of
406 carrying capacities for some bacterial orders, or non-constant or non-homogeneous
407 variance-covariance matrices (e.g., more frequent shifts in microbiota composition
408 early in clades history, effects of host traits such as diet or gut pH on covariation).
409 Extensions of our multivariate Brownian motion approach could accommodate such
410 constraints, but this may complexify inferences. We hope that this work will foster the
411 development of more complex models that may better represent microbiota evolution
412 in systems that present non-Brownian behaviors. As a first step, extensions that relax
413 the constant variance assumption (e.g., the early-burst model; Harmon et al. 2010)
414 would be relatively straightforward to implement and could be particularly relevant to
415 account for the major shifts in microbiota composition that took place at the origin of
416 some mammalian orders (e.g., in bats). Meanwhile, by relying on a simple and flexible
417 Brownian motion process, our phylogenetic comparative model for microbiota

418 evolution is general enough to be broadly applied across other host-microbiota
419 systems and reveal the global trends of microbiota evolution.

420

421 Besides modeling assumptions, our results may be influenced by the inherent
422 biases of metabarcoding data. Bacterial relative abundances characterized using
423 metabarcoding techniques are a distortion of the actual relative abundances (Knight et
424 al. 2018; Lavrinienko et al. 2021), since metabarcoding is sensitive to the number of
425 rRNA copies in the bacterial genomes, primer biases, and the quality and
426 completeness of the reference database for taxonomic assignment (at the bacterial
427 order/phylum level in our case). These issues are unlikely to artifactually generate
428 phylosymbiosis or covariations across bacterial taxa because we expect such biases
429 to be homogeneous across host species; nevertheless, they are likely to affect our
430 ancestral reconstructions of microbiota compositions.

431

432 Our approach to quantifying phylosymbiosis characterizes microbiota
433 composition in terms of the relative abundances of higher bacterial taxa (orders or
434 phyla). This characterization hides variations in the presence/absence of bacterial taxa
435 at lower taxonomic levels (e.g. genus or species). Indeed, distinct mammal or bird
436 species are known to host different bacterial species (Song et al. 2020), and this may
437 not translate into abundance variations at higher taxonomic levels if the different
438 bacterial species belong to the same higher taxa. Besides the widely-used Mantel
439 tests, such variations could be accounted for by stochastic processes modeling the
440 evolution of presence/absence on host phylogenies (Braga et al. 2020), although we
441 are not aware that these approaches have been used to detect bacterial
442 phylosymbiosis. Yet another level of variation in microbiota composition that can
443 contribute to phylosymbiosis arises through genetic differentiation below the bacterial
444 species level: if a bacterial species is vertically transmitted during host diversification,
445 we expect bacterial strains from closely related host species to be more genetically
446 similar (Sanders et al. 2014; Groussin et al. 2017; Perez-Lamarque and Morlon 2019).
447 This latter process can be specifically tested thanks to cophylogenetic methods that
448 consider the evolution of each microbial species separately (Dismukes et al. 2022;
449 Perez-Lamarque and Morlon 2022). The above-mentioned methods are
450 complementary, as they focus on different levels of variations in microbiota
451 composition, and on the distinct processes that simultaneously generate
452 phylosymbiosis (Moran et al. 2019; Lim and Bordenstein 2020).

453

454 Phylosymbiosis is a widespread pattern that has fascinated microbial ecologists
455 and evolutionary biologists since its discovery, spurring debates on the main processes
456 underlying the pattern. Drawing upon phylogenetic comparative methods, we have
457 developed a new approach to studying phylosymbiosis. Our results on simulations and
458 birds suggest that phylosymbiosis may be even more prevalent than currently
459 recognized, but sometimes undetected with correlative approaches. We have shown
460 that conservatisms in diet, geographic location, and flying ability are not enough to
461 explain phylosymbiosis, calling for an investigation of the role of other host ecological

462 traits, as well as physiological and immunological traits. One of our most striking
463 results, in the face of the well-known high variability of the gut microbiota, is its high
464 level of integration, with conserved covariations between bacterial orders over millions
465 of years. The same two subsets of bacterial orders tend to covary in a concerted way
466 in both mammals and birds, leading to the existence of two main gut microbiota profiles
467 in vertebrates. Hence, microbial interactions combined with phylogenetically-
468 conserved host traits shape microbiota composition over millions of years, supporting
469 the view of vertebrate gut microbiota as 'ecosystems on a leash' (Foster et al. 2017).

470 **Methods:**

471

472 **A multivariate Brownian motion model for variations in microbiota composition**
473 **over host evolutionary time:**

474

475 We denote by p the total number of microbial taxa detected across the
476 microbiota of the n sampled host species. Standard metabarcoding techniques only
477 measure the relative abundance of each microbial taxon j in each extant host species
478 i , which we denote by $Z_{ij} = X_{ij}/Y_i$, where X_{ij} is the unmeasured absolute abundance
479 of microbial taxon j in host i and $Y_i = \sum_j X_{ij}$ is the unmeasured total microbial
480 abundance in the microbiota of host i . We assume that the logarithms of microbial
481 absolute abundances $\log X_{ij}$ vary along the host phylogenetic tree according to a
482 multivariate Brownian motion starting from the ancestral abundances at the root,
483 denoted by X_{0j} (Figure 1). Indeed, taking the logarithm of the abundances yields values
484 on the real axis that are amenable to be modeled with a Brownian motion, similar to
485 continuous phenotypic traits. This model implies a log-normal distribution of
486 abundances, as is commonly observed in microbial communities (Quince et al. 2008),
487 and it can easily accommodate undetected microbial taxa in some hosts by assigning
488 them very low unobserved relative abundances. To make the model identifiable, we
489 express the total abundances Y_i relative to the unknown total abundance at the root Y_0 ,
490 and we only infer $\tilde{Y}_i = Y_i/Y_0$. Each microbial taxon i is characterized by a certain
491 variance and pairs of microbial taxa can affect each other through a covariance term,
492 so that their changes in abundance over time can be positively or negatively correlated.
493 All variance and covariance values are assumed to be constant along the host
494 phylogeny and are summarized by the invertible variance-covariance matrix R (Figure
495 1a).

496

497 **Model inference:**

498

499 To infer the model parameters, we sampled from their joint posterior distribution
500 $P(\log Z_0, R, \lambda, \log \tilde{Y}_1, \dots, \log \tilde{Y}_n | Z_{11}, \dots, Z_{ij}, \dots, Z_{np}, C)$ using a No U-turn Hamiltonian
501 Monte Carlo sampler, a computationally efficient Markov Chain Monte Carlo algorithm
502 for continuous variables (Supplementary Methods 1). We implemented it in the
503 probabilistic programming language Stan and we ran and compiled it through the
504 RStan interface (R Core Team 2022; Stan Development Team 2022). Inferences were
505 performed with 4 independent chains and a minimum of 4,000 iterations per chain
506 including a warmup of 2,000 iterations. We checked the convergence of the chains
507 using the Gelman statistics and effective sample sizes (ESS). We extracted the mean
508 posterior value of each parameter and its associated 95% credible interval across
509 posterior samples.

510

511 We considered a covariance to be significant if 0 was not included in its 95%
512 credible interval. We could not use the same approach for λ , because it only takes

513 positive values. Furthermore, model selection using Bayes factors led to many false
514 negatives on simulated data (Supplementary Methods 2 & Results 1). Therefore, we
515 assessed the significance of λ using permutations. We shuffled at random the extant
516 host species to break the phylogenetic structure and ran again model inference of the
517 randomized dataset. We performed 100 replications and compared the distribution of
518 λ values thus obtained to the original λ estimate: if the original λ was greater than at
519 least 95% of the λ values obtained through permutations, we considered that there
520 was a significant impact of host evolution on microbiota evolution.

521

522 **Simulations:**

523

524 We evaluated our approach using simulations. We simulated the evolution of a
525 microbiota along a host phylogeny using Multivariate Brownian motions for log-
526 abundances. We simulated phylogenies with $n = 20, 50, 100,$ or 250 extant host
527 species using a pure birth model (*pbtree* function in the phytools R-package (Revell
528 2012)). We considered microbiota with $p = 3, 5, 10,$ or 15 microbial taxa and uniformly
529 sampled the logarithms of their ancestral abundances at the root of the host phylogeny
530 between -4 and 0 before normalizing them so that $\sum_j Z_{0j} = 1$. We generated random
531 positive definite variance-covariance matrices R following (Uyeda et al. 2015) and
532 (Clavel et al. 2019) with eigenvalues of $1/4$. Finally, we applied Pagel's λ
533 transformations with $\lambda = 1, 0.75, 0.5, 0.25,$ or 0 . For each combination of $n, p,$ and λ
534 values, we performed 100 independent simulations, leading to a total of 8,000
535 simulations. We verified that our approach correctly estimates the parameters $\lambda, Z_0,$
536 and R , and detects phylosymbiosis (significant λ) and covariations (significant R
537 components) when they are simulated. We compared the performances of our
538 approach for detecting phylosymbiosis to that of Mantel tests (Perez-Lamarque, Maliet,
539 et al. 2022).

540

541 We also evaluated our inference approach using data simulated on the
542 phylogenetic tree of mammals or birds, and using conditions and parameters matching
543 the empirical data. We performed simulations with 7 taxa (corresponding to the 7
544 bacterial phyla in the data, see below) and 14 taxa (corresponding to the 14 bacterial
545 orders in the data). We used values of $\lambda = 1, 0.75, 0.5, 0.25,$ or 0 , and values for the
546 other model parameters similar to those estimated from the empirical data (Figure
547 S13). We performed 100 simulations per condition (thus reaching a total of 2,000
548 simulations).

549

550 **Empirical application:**

551

552 We downloaded the dataset of (Song et al. 2020) that gathered the gut microbiota of
553 2,677 mammal individuals from >200 species and 1,630 bird individuals from >300
554 species, characterized by metabarcoding using the V4 region of the 16S rRNA gene.
555 Only studies using the standard protocol of the Earth Microbiome Project (Thompson

556 et al. 2017) were included (see (Song et al. 2020) for details), making samples
557 comparable across different studies (Knight et al. 2018). Song *et al.* converted bacterial
558 reads into amplicon sequence variants (ASV), assigned each ASV taxonomically using
559 the Greengenes database (DeSantis et al. 2006; Song et al. 2020), and rarefied ASV
560 tables at 10,000 reads per sample. We complemented their dataset with the consensus
561 phylogenetic trees of (Upham et al. 2019) and (Jetz et al. 2012) for mammals and
562 birds, respectively. We only kept the species having their microbiota compositions
563 characterized by at least 2 microbiota samples (Table S2). We checked that gut
564 microbiota from the same host species were more similar than gut microbiota from
565 different species using PerMANOVA (Oksanen et al. 2016). Then, we obtained the
566 microbiota composition of each host species by averaging the samples per species
567 and extracted the relative abundances of the main bacterial orders and phyla per host
568 species. We verified that similar results were obtained when repeating our analyses by
569 randomly sampling one individual per host species (Figure S14). We only considered
570 the 14 most abundant bacterial orders, *i.e.* those that each represented more than 1%
571 of the total bacterial abundance (which correspond in abundance to 84% and 82% of
572 the total gut bacterial microbiota of mammals and birds, respectively) and the 7 most
573 abundant bacterial phyla (95% and 96% of the gut microbiota of mammals and birds
574 respectively; Figure S15). We also repeated all analyses using only the 9 (resp. 5)
575 most abundant orders (resp. phyla). We did not apply our model at lower taxonomic
576 levels mainly because the assumptions of our model (all microbial taxa are present in
577 all hosts, potentially in undetectable abundances and they were already present in the
578 most recent common ancestor of all host species) are more likely to be met at high
579 taxonomic levels. At lower taxonomic levels, the microbiota evolution of mammals and
580 birds may be better represented using models of colonization and extinction (Song et
581 al. 2020) than models of fluctuations in bacterial abundances such as ours. In addition,
582 running the model with several hundreds of taxa would be computationally intensive.
583 Finally, the quality of the taxonomic assignation and the number of taxa representing
584 more than 1% of the gut microbiota decreased sharply at low taxonomic levels: only
585 81% and 45% of the gut microbiota of mammals and birds are assigned at the family
586 and genus levels, respectively, and among them, only 60% and 18% of the bacterial
587 taxa represent more than 1% of the gut microbiota.

588
589 Our multivariate Brownian motion model of microbiota does not explicitly
590 consider losses of bacterial taxa from the microbiota through time. Yet, some bacterial
591 taxa can be absent or undetected in the gut microbiota of mammals and birds. We
592 assumed that the absence of a particular taxon came from a very low abundance,
593 below the detection threshold: we thus arbitrarily set the relative abundances of absent
594 taxa to 0.001%. Setting the minimal relative abundances of absent taxa to 0.01%
595 reduced the estimated variance of the rare taxa but did not affect other estimates
596 (Figure S16).

597

598 We applied the model separately on all mammals and all birds, getting estimates
599 of Pagel's λ , the ancestral microbiota composition Z_0 , and the variance-covariance
600 matrix R for each vertebrate class.

601

602 **Effect of host traits on phylosymbiosis:**

603

604 We gathered data on host species traits from (Song et al. 2020) for diet,
605 geographic location, and flying ability. We assigned a dominant diet to each host
606 species as either "plants", "fruits", "invertebrates" or "meat" following the EltonTraits
607 database (Wilman et al. 2014). We assigned a geographic location to each species by
608 picking the biogeographic realm (Afrotropical, Antarctic, Australasian, Nearctic,
609 Neotropic, Oriental, or Palearctic) where the highest number of wild individuals were
610 sampled, or if not available, where the highest number of captive individuals were
611 sampled (this was the case for 48% of the mammalian species and 18% of the avian
612 ones). We treated flying ability as binary (yes/no). First, we assessed the influence of
613 flight on the gut microbiota by performing inferences on non-flying mammal species
614 only (*i.e.* excluding bats) and on flying bird species only. Similarly, we investigated the
615 effect of captivity on our inferences by replicating them using only the gut microbiota
616 of wild or captive individuals. Second, we tested whether the evolutionary conservatism
617 of diet, geographic location, or flying ability may explain phylosymbiosis in mammals
618 and birds by performing permutations. We shuffled host species having the same diet,
619 geographic location, and/or flying ability and re-ran the inferences on these
620 randomized datasets. For each tested trait, we performed 100 independent
621 randomizations. Finally, we verified that phylosymbiosis did not artefactually arise from
622 the concatenation of the separate studies composing this dataset by randomizing the
623 species that came from the same study.

624

625 **Comparison between ancestral and present-day microbiota composition:**

626

627 We compared the estimated ancestral microbiota composition Z_0 of all
628 mammals or birds to that of extant species using principal component analysis (PCA)
629 after applying a centered log-ratio transform to the abundances (Aitchison 1983).
630 Given Z_0 , we also jointly estimated the ancestral abundances at each node of the host
631 phylogenetic tree using generalized least squares following (Martins and Hansen 1997;
632 Cunningham et al. 1998; Clavel et al. 2019). As a first attempt to infer past diet based
633 on the estimated ancestral microbiota composition Z_0 , we computed the centroid of
634 each of the four diet categories and computed the distance d_i between Z_0 and each
635 centroid on the first five PC axes. We additionally performed separate model inference
636 for all orders of mammals (Carnivora, Cetartiodactyla, Chiroptera, Primates, and
637 Rodentia; Table S2) and birds (Anseriformes, Charadriiformes, Columbiformes, and
638 Passeriformes) represented by at least 15 species, and compared the ancestral
639 microbiota composition obtained with separate and joint inferences.

640

641 **Integration analyses:**

642

643 We identified the significantly positive or negative covariances between
644 bacterial orders. In addition, to characterize potential subsets of bacterial taxa that tend
645 to vary in a concerted way, we clustered taxa using the *cluster_fast_greedy* function in
646 the R-package *igraph* (Csardi and Nepusz 2006), based on the estimated variance-
647 covariance matrix R , modified to retain information of only positive covariances
648 (negative ones were set to 0).

649

650 **Model adequacy:**

651

652 To assess whether our model for the evolution of the gut microbiota of mammals and
653 birds yields realistic microbiota compositions, we simulated the process of microbiota
654 evolution on the mammal or bird phylogenies using the parameters estimated for
655 mammals and birds ($\log Z_0$, R , and λ). Next, we compared the simulated microbiota
656 compositions to the empirical microbiota compositions of the extant mammal or bird
657 species using principal component analysis (PCA). We performed 20 independent
658 simulations for each of our model inferences.

659

660 **Data availability:**

661

662 Raw data and processed data from (Song et al. 2020) used to perform the empirical
663 applications are available in Qiita (<https://qiita.ucsd.edu/study/description/11166>).

664 Our phylogenetic comparative method, referred to as ABDOMEN (A Brownian moDel
665 Of Microbiota Evolution), is available on GitHub with a tutorial:
666 <https://github.com/BPerezLamarque/ABDOMEN>.

667

668 **Acknowledgments:**

669

670 The authors acknowledge Julien Clavel, Jonathan Drury, Félix Foutel--Rodier, and
671 members of the BioDiv team at IBENS for helpful discussions, as well as the Editor
672 Aurélien Tellier and two anonymous reviewers for their constructive comments. They
673 also acknowledge the Hubert Curien Alliance program for funding workshops that
674 initiated the project. GSK acknowledges support from the Academy of Finland
675 (decision 340314) and the Sakari Alhopuro foundation (grant 20210172). This work
676 was performed using HPC resources from GENCI-IDRIS (Grants 2021-A0100312405
677 and 2022- AD010313735).

678

679 **Author Contributions:**

680

681 BPL, GSK, LD, and HM designed the study. BPL and GSK implemented the model.
682 BPL performed the simulations and the empirical applications. BPL, GSK, and HM
683 wrote the manuscript.

684

685 **Declaration of interests:**

686

687 The authors declare no competing interests.

688

689 **References:**

690

691 Aitchison J. 1983. Principal component analysis of compositional data. *Biometrika*
692 70:57.

693 Amato KR, G. Sanders J, Song SJ, Nute M, Metcalf JL, Thompson LR, Morton JT,
694 Amir A, J. McKenzie V, Humphrey G, et al. 2019. Evolutionary trends in host
695 physiology outweigh dietary niche in structuring primate gut microbiomes. *ISME*
696 *J.* 13:576–587.

697 Bodawatta KH, Hird SM, Grond K, Poulsen M, Jønsson KA. 2022. Avian gut
698 microbiomes taking flight. *Trends Microbiol.* 30:268–280.

699 Braga MP, Landis MJ, Nylín S, Janz N, Ronquist F. 2020. Bayesian inference of
700 ancestral host-parasite interactions under a phylogenetic model of host
701 repertoire evolution. *Syst. Biol.* 69:1149–1162.

702 Brooks AW, Kohl KD, Brucker RM, van Opstal EJ, Bordenstein SR. 2016.
703 *Phylosymbiosis: relationships and functional effects of microbial communities*
704 *across host evolutionary history.* Relman D, editor. *PLOS Biol.* 14:e2000225.

705 Capuntan DC, Johnson O, Terrill RS, Hird SM. 2020. Evolutionary signal in the gut
706 microbiomes of 74 bird species from Equatorial Guinea. *Mol. Ecol.* 29:829–847.

707 Clavel J, Aristide L, Morlon H. 2019. A penalized likelihood framework for high-
708 dimensional phylogenetic comparative methods and an application to New-
709 World monkeys brain evolution. *Syst. Biol.* 68:93–116.

710 Clavel J, Escarguel G, Merceron G. 2015. mvMORPH: An R package for fitting
711 multivariate evolutionary models to morphometric data. Poisot T, editor. *Methods*
712 *Ecol. Evol.* 6:1311–1319.

713 Csardi G, Nepusz T. 2006. The igraph software package for complex network
714 research. *InterJournal Complex Syst. Complex Sy:*1695.

715 Cunningham CW, Omland KE, Oakley TH. 1998. Reconstructing ancestral character
716 states: a critical reappraisal. *Trends Ecol. Evol.* 13:361–366.

717 David LA, Maurice CF, Carmody RN, Gootenberg DB, Button JE, Wolfe BE, Ling A
718 V., Devlin AS, Varma Y, Fischbach MA, et al. 2014. Diet rapidly and reproducibly
719 alters the human gut microbiome. *Nature* 505:559–563.

720 DeSantis TZ, Hugenholtz P, Larsen N, Rojas M, Brodie EL, Keller K, Huber T, Dalevi
721 D, Hu P, Andersen GL. 2006. Greengenes, a chimera-checked 16S rRNA gene
722 database and workbench compatible with ARB. *Appl. Environ. Microbiol.*
723 72:5069–5072.

724 Dion-Phénix H, Charmantier A, de Franceschi C, Bourret G, Kembel SW, Réale D.
725 2021. Bacterial microbiota similarity between predators and prey in a blue tit
726 trophic network. *ISME J.* 15:1098–1107.

727 Dismukes W, Braga MP, Hembry DH, Heath TA, Landis MJ. 2022. Cophylogenetic
728 methods to untangle the evolutionary history of ecological interactions. *Annu.*
729 *Rev. Ecol. Evol. Syst.* 53:1–24.

730 Eriksson O. 2016. Evolution of angiosperm seed disperser mutualisms: The timing of
731 origins and their consequences for coevolutionary interactions between

732 angiosperms and frugivores. *Biol. Rev.* 91:168–186.

733 Faust K, Sathirapongsasuti JF, Izard J, Segata N, Gevers D, Raes J, Huttenhower C.
734 2012. Microbial co-occurrence relationships in the human microbiome. Ouzounis
735 CA, editor. *PLoS Comput. Biol.* 8:e1002606.

736 Foster KR, Schluter J, Coyte KZ, Rakoff-Nahoum S. 2017. The evolution of the host
737 microbiome as an ecosystem on a leash. *Nature* 548:43–51.

738 Gill PG, Purnell MA, Crumpton N, Brown KR, Gostling NJ, Stampanoni M, Rayfield
739 EJ. 2014. Dietary specializations and diversity in feeding ecology of the earliest
740 stem mammals. *Nature* 512:303–305.

741 Goodrich JK, Davenport ER, Waters JL, Clark AG, Ley RE. 2016. Cross-species
742 comparisons of host genetic associations with the microbiome. *Science* (80-).
743 352:532–535.

744 Grossnickle DM, Smith SM, Wilson GP. 2019. Untangling the multiple ecological
745 radiations of early mammals. *Trends Ecol. Evol.* 34:936–949.

746 Groussin M, Mazel F, Sanders JG, Smillie CS, Lavergne S, Thuiller W, Alm EJ. 2017.
747 Unraveling the processes shaping mammalian gut microbiomes over
748 evolutionary time. *Nat. Commun.* 8:14319.

749 Hacquard S, Garrido-Oter R, González A, Spaepen S, Ackermann G, Lebeis S,
750 McHardy AC, Dangl JL, Knight R, Ley R, et al. 2015. Microbiota and host
751 nutrition across plant and animal kingdoms. *Cell Host Microbe* 17:603–616.

752 Harmon LJ. 2017. *Phylogenetic Comparative Methods*.

753 Harmon LJ, Glor RE. 2010. Poor statistical performance of the Mantel test in
754 phylogenetic comparative analyses. *Evolution* (N. Y). 64:2173–2178.

755 Harmon LJ, Losos JB, Jonathan Davies T, Gillespie RG, Gittleman JL, Bryan
756 Jennings W, Kozak KH, McPeck MA, Moreno-Roark F, Near TJ, et al. 2010.
757 Early bursts of body size and shape evolution are rare in comparative data.
758 *Evolution* (N. Y). 64:2385–2396.

759 Hird SM. 2019. Microbiomes, community ecology, and the comparative method.
760 *mSystems* 4:1–5.

761 Hird SM, Sánchez C, Carstens BC, Brumfield RT. 2015. Comparative Gut Microbiota
762 of 59 Neotropical Bird Species. *Front. Microbiol.* 6:1403.

763 Jetz W, Thomas GH, Joy JB, Hartmann K, Mooers AO. 2012. The global diversity of
764 birds in space and time. *Nature* 491:444–448.

765 Knight R, Vrbanac A, Taylor BC, Aksenov A, Callewaert C, Debelius J, Gonzalez A,
766 Kosciolk T, McCall LI, McDonald D, et al. 2018. Best practices for analysing
767 microbiomes. *Nat. Rev. Microbiol.* 16:410–422.

768 Kohl KD. 2020. Ecological and evolutionary mechanisms underlying patterns of
769 phyllosymbiosis in host-associated microbial communities. *Philos. Trans. R. Soc.*
770 *B Biol. Sci.* 375:20190251.

771 Kohl KD, Dearing MD, Bordenstein SR. 2018. Microbial communities exhibit host
772 species distinguishability and phyllosymbiosis along the length of the
773 gastrointestinal tract. *Mol. Ecol.* 27:1874–1883.

774 Labrador M del M, Doña J, Serrano D, Jovani R. 2021. Quantitative interspecific
775 approach to the stylosphere: Patterns of bacteria and fungi abundance on
776 passerine bird feathers. *Microb. Ecol.* 81:1088–1097.

777 Lavrinienko A, Jernfors T, Koskimäki JJ, Pirttilä AM, Watts PC. 2021. Does
778 intraspecific variation in rDNA copy number affect analysis of microbial
779 communities? *Trends Microbiol.* 29:19–27.

780 Ley RE, Lozupone CA, Hamady M, Knight R, Gordon JI. 2008. Worlds within worlds:
781 evolution of the vertebrate gut microbiota. *Nat. Rev. Microbiol.* 6:776–788.

782 Lim SJ, Bordenstein SR. 2020. An introduction to phyllosymbiosis. *Proc. R. Soc. B*
783 *Biol. Sci.* 287:20192900.

784 Martins EP, Hansen TF. 1997. Phylogenies and the comparative method: A general
785 approach to incorporating phylogenetic information into the analysis of
786 interspecific data. *Am. Nat.* 149:646–667.

787 Mazel F, Davis KM, Loudon A, Kwong WK, Groussin M, Parfrey LW. 2018. Is host
788 filtering the main driver of phyllosymbiosis across the Tree of Life? Bik H, editor.
789 *mSystems* 3:1–15.

790 McFall-Ngai M, Hadfield MG, Bosch TCG, Carey H V., Domazet-Lošo T, Douglas
791 AE, Dubilier N, Eberl G, Fukami T, Gilbert SF, et al. 2013. Animals in a bacterial
792 world, a new imperative for the life sciences. *Proc. Natl. Acad. Sci.* 110:3229–
793 3236.

794 Mirpuri J, Raetz M, Sturge CR, Wilhelm CL, Benson A, Savani RC, Hooper L V,
795 Yarovinsky F. 2013. Proteobacteria-specific IgA regulates maturation of the
796 intestinal microbiota. *Gut Microbes* 5:28–39.

797 Moran NA, Ochman H, Hammer TJ. 2019. Evolutionary and ecological
798 consequences of gut microbial communities. *Annu. Rev. Ecol. Evol. Syst.*
799 50:451–475.

800 Nishida AH, Ochman H. 2018. Rates of gut microbiome divergence in mammals.
801 *Mol. Ecol.* 27:1884–1897.

802 Ochman H, Worobey M, Kuo CH, Ndjango JBN, Peeters M, Hahn BH, Hugenholtz P.
803 2010. Evolutionary relationships of wild hominids recapitulated by gut microbial
804 communities. *PLoS Biol.* 8:3–10.

805 Oksanen J, Kindt R, Pierre L, O’Hara B, Simpson GL, Solymos P, Stevens MH. HH,
806 Wagner H, Blanchet FG, Kindt R, et al. 2016. *vegan: Community Ecology*
807 *Package, R package version 2.4-0. R Packag. version 2.2-1.*

808 Pagel M. 1999. Inferring the historical patterns of biological evolution. *Nature*
809 401:877–884.

810 Perez-Lamarque B, Krehenwinkel H, Gillespie RG, Morlon H. 2022. Limited evidence
811 for microbial transmission in the phyllosymbiosis between Hawaiian spiders and
812 their microbiota. Hird SM, editor. *mSystems* 7:e01104-21.

813 Perez-Lamarque B, Maliet O, Pichon B, Selosse M-A, Martos F, Morlon H. 2022. Do
814 closely related species interact with similar partners? Testing for phylogenetic
815 signal in bipartite interaction networks. *Peer Community J.* 2:e59.

816 Perez-Lamarque B, Morlon H. 2019. Characterizing symbiont inheritance during
817 host–microbiota evolution: Application to the great apes gut microbiota. *Mol.*
818 *Ecol. Resour.* 19:1659–1671.

819 Perez-Lamarque B, Morlon H. 2022. Comparing different computational approaches
820 for detecting long-term vertical transmission in host-associated microbiota. *Mol.*
821 *Ecol.*

822 Pigliucci M. 2003. Phenotypic integration: Studying the ecology and evolution of
823 complex phenotypes. *Ecol. Lett.* 6:265–272.

824 Quince C, Curtis TP, Sloan WT. 2008. The rational exploration of microbial diversity.
825 *ISME J.* 2:997–1006.

826 R Core Team. 2022. *R: A language and environment for statistical computing.*

827 Revell LJ. 2012. *phytools: An R package for phylogenetic comparative biology (and*
828 *other things).* *Methods Ecol. Evol.* 3:217–223.

829 Revell LJ, Harmon LJ, Collar DC. 2008. Phylogenetic signal, evolutionary process,
830 and rate. *Syst. Biol.* 57:591–601.

831 Sanders JG, Powell S, Kronauer DJC, Vasconcelos HL, Frederickson ME, Pierce

832 NE. 2014. Stability and phylogenetic correlation in gut microbiota: lessons from
833 ants and apes. *Mol. Ecol.* 23:1268–1283.

834 Shealy NG, Yoo W, Byndloss MX. 2021. Colonization resistance: metabolic warfare
835 as a strategy against pathogenic Enterobacteriaceae. *Curr. Opin. Microbiol.*
836 64:82–90.

837 Shin NR, Whon TW, Bae JW. 2015. Proteobacteria: Microbial signature of dysbiosis
838 in gut microbiota. *Trends Biotechnol.* 33:496–503.

839 Song SJ, Sanders JG, Delsuc F, Metcalf J, Amato K, Taylor MW, Mazel F, Lutz HL,
840 Winker K, Graves GR, et al. 2020. Comparative analyses of vertebrate gut
841 microbiomes reveal convergence between birds and bats. *MBio* 11:1–14.

842 Stan Development Team. 2022. RStan: the R interface to Stan.

843 Thompson LR, Sanders JG, McDonald D, Amir A, Ladau J, Locey KJ, Prill RJ,
844 Tripathi A, Gibbons SM, Ackermann G, et al. 2017. A communal catalogue
845 reveals Earth’s multiscale microbial diversity. *Nature* 551:457–463.

846 Trevelline BK, Sosa J, Hartup BK, Kohl KD. 2020. A bird’s-eye view of
847 phyllosymbiosis: weak signatures of phyllosymbiosis among all 15 species of
848 cranes. *Proc. R. Soc. B Biol. Sci.* 287:20192988.

849 Upham NS, Esselstyn JA, Jetz W. 2019. Inferring the mammal tree: Species-level
850 sets of phylogenies for questions in ecology, evolution, and
851 conservation. Tanentzap AJ, editor. *PLoS Biol.* 17:e3000494.

852 Uyeda JC, Caetano DS, Pennell MW. 2015. Comparative analysis of principal
853 components can be misleading. *Syst. Biol.* 64:677–689.

854 Wagner MR, Lundberg DS, Del Rio TG, Tringe SG, Dangl JL, Mitchell-Olds T. 2016.
855 Host genotype and age shape the leaf and root microbiomes of a wild perennial
856 plant. *Nat. Commun.* 7:12151.

857 Wilman H, Belmaker J, Simpson J, de la Rosa C, Rivadeneira MM, Jetz W. 2014.
858 EltonTraits 1.0: Species-level foraging attributes of the world’s birds and
859 mammals. *Ecology* 95:2027–2027.

860